



Thermochronological constraints of the exhumation and uplift of the Sierra de Pie de Palo, NW Argentina

Stefan Löbens*, Frithjof A. Bense, István Dunkl, Klaus Wemmer, Jonas Kley,
Siegfried Siegesmund

Geoscience Centre, University of Göttingen, Goldschmidtstr. 3, 37077 Göttingen, Germany



ARTICLE INFO

Article history:

Received 15 November 2012
Accepted 11 September 2013

Keywords:

Exhumation
Uplift
Thermochronology
Sierra de Pie de Palo
Argentina

ABSTRACT

The Sierra de Pie de Palo located between 67°30'–68°30' W and 31°00'–32°00' S in the Argentine Western Sierras Pampeanas in Argentina is a distinct basement range, which lacks thermochronological data deciphering its exhumation and uplift history below 200 °C. Integrated cooling histories constrained by apatite fission-track data as well as (U-Th)/He measurements of zircon and apatite reveal that the structural evolution of this mountain range commenced during the Late Paleozoic and was mainly controlled by tectonically triggered erosion. Following further erosional controlled exhumation in a more or less extensional regime during the Mesozoic, the modern topography was generated by denudation in the Paleogene during the early stage of the Andean deformation, whereupon deformation propagated towards the west since the Late Mesozoic to Paleogene. This evolution is characterised by a total of 3.7–4.2 km vertical rock uplift and by 1.7–2.2 km exhumation with a rate of 0.03–0.04 mm/a within the Sierra de Pie de Palo since ca. 60 Ma. Onset of uplift of peak level is also referred to that time resulting in a less Pliocene amount of uplift than previously assumed.

© 2013 Elsevier Ltd. All rights reserved.

1. Introduction

Most recent geochronological studies of the western margin of the Sierras Pampeanas in western Argentina are concerned to terrane-related accretional history at the southwestern proto-Andean margin of Gondwana and the accompanying metamorphic evolution during the Paleozoic (e.g. Casquet et al., 2001; Morata et al., 2010; Mulcahy et al., 2007; Pankhurst and Rapela, 1998; Ramos et al., 1998; Varela and Dalla Salda, 1992; Varela et al., 2011; Vujovich et al., 2004). One of these terranes is represented by the Cuyania Terrane which is bounded by the Pampean Terrane to the east, the Chilenia Terrane in the west and the Famatinia Terrane to the north (Fig. 1; e.g. Ramos et al., 2002; Ramos and Vujovich, 2000). The origin and accretion of the Cuyania Terrane, which comprises the Western Sierras Pampeanas (sensu Caminos, 1979) including the Sierra de Pie de Palo, during the Ordovician is still controversially discussed in the literature (e.g. Aceñolanza and Toselli, 1988; Finney et al., 2003; Meira et al., 2012; Mulcahy et al., 2007; Ramos, 1988, 2004; Ramos et al., 1998; Thomas and Astini, 2003; van Staal et al., 2011). On one hand, most authors agree that the exotic Cuyania, or Precordillera Terrane

represents an allochthonous continental block derived from Laurentia and accreted to the southwestern proto-Andean margin of Gondwana during the Famatinian orogenic cycle in Middle Ordovician (e.g. Ramos, 1988, 2004; Ramos et al., 1998; Thomas and Astini, 2003) or Silurian/Devonian times (e.g. Keller et al., 1998; Pankhurst and Rapela, 1998; Rapela et al., 1998). On the other hand, the Cuyania Terrane is considered to be of paraautochthonous Gondwanan origin displaced along a strike-slip fault at the southern margin of West Gondwana (present situation, e.g. Aceñolanza and Toselli, 1988; Baldis et al., 1989; Finney et al., 2003).

The Cenozoic evolution of the most western basement uplifts of the Sierras Pampeanas, which is mainly associated with the Andean deformation (e.g. Ramos et al., 2002), was usually investigated using geophysical, structural, and lithological approaches (e.g. Jordan and Allmendinger, 1986; Ramos and Vujovich, 2000; Regnier et al., 1992). However, low-temperature thermochronological data, i.e. fission-track and (U-Th)/He dating of apatite, providing constraints on amount of cooling/erosion related to mountain building, crustal deformation, extensional tectonics as well as landscape evolution (e.g. Farley, 2002; Fitzgerald et al., 2006; Gallagher et al., 1998; Stockli et al., 2000) are still scarce within this region. Coughlin et al. (1998) reported apatite fission-track measurements for the Sierra de Valle Fértil, Sierra de La Maz, and Sierra Umango suggesting that deformation in the Sierras Pampeanas could be associated with uplift of the Puna Plateau

* Corresponding author. Tel.: +49 551 399375.

E-mail address: stefan.loebens@geo.uni-goettingen.de (S. Löbens).

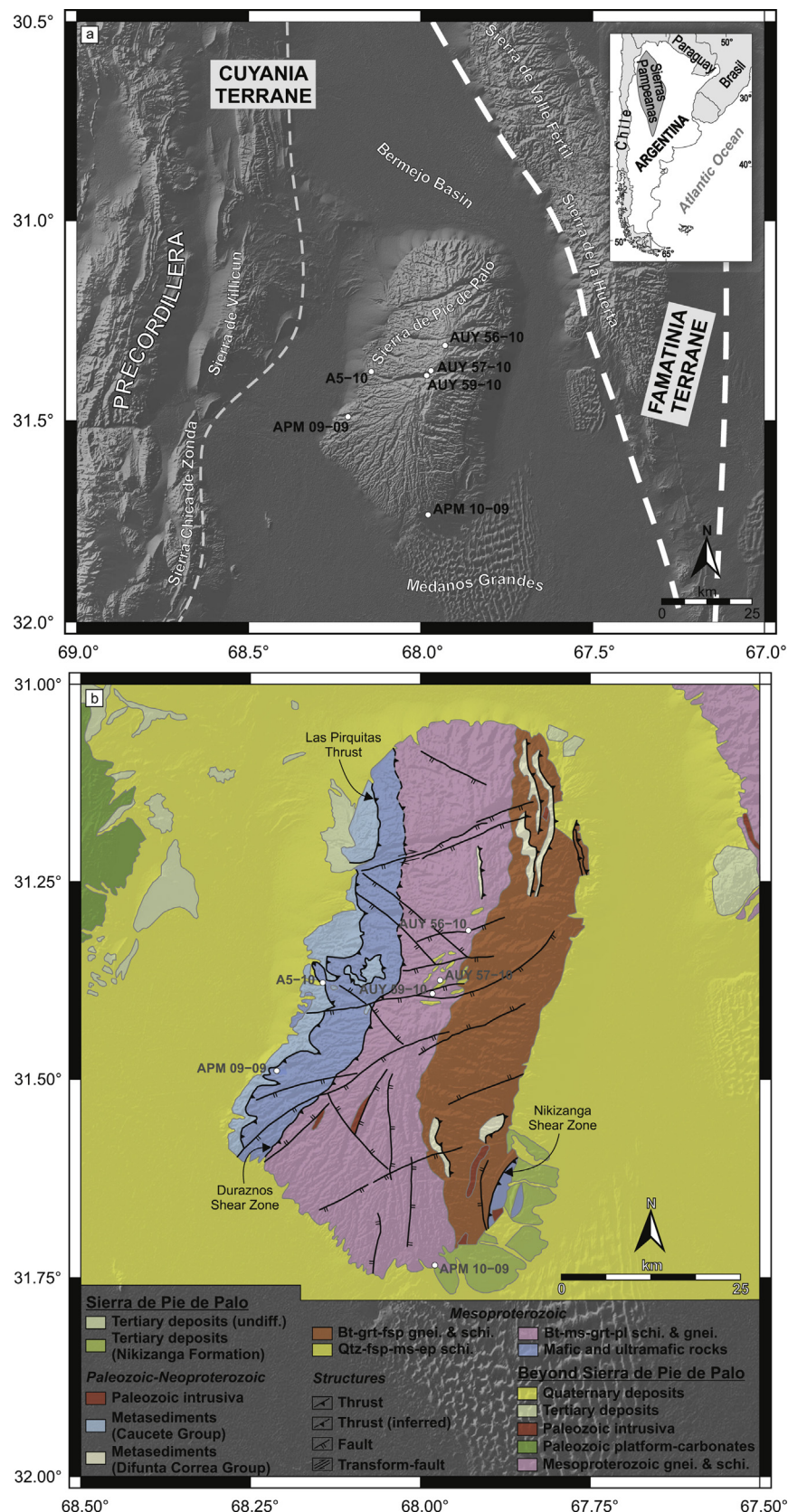


Fig. 1. Overview of the study area. a) SRTM-3 digital elevation model showing morphostructural features in the western part of the Argentine Sierras Pampeanas including the Sierra de Pie de Palo and the localities of samples. White dashed lines mark the boundary between different terranes accreted during the Paleozoic (from Ramos (2004)); grey dashed line defines the boundary between the Precordillera and the Western Sierras Pampeanas (from Giambiagi and Martínez (2008)). The schematic inset in upper right shows the study area on the South American continent. b) Simplified geological map of the Sierra de Pie de Palo according to the 1:250,000 geological maps of Ramos and Vujovich (2000) and Varela et al. (2011); schi. = schists, gnei. = gneisses.

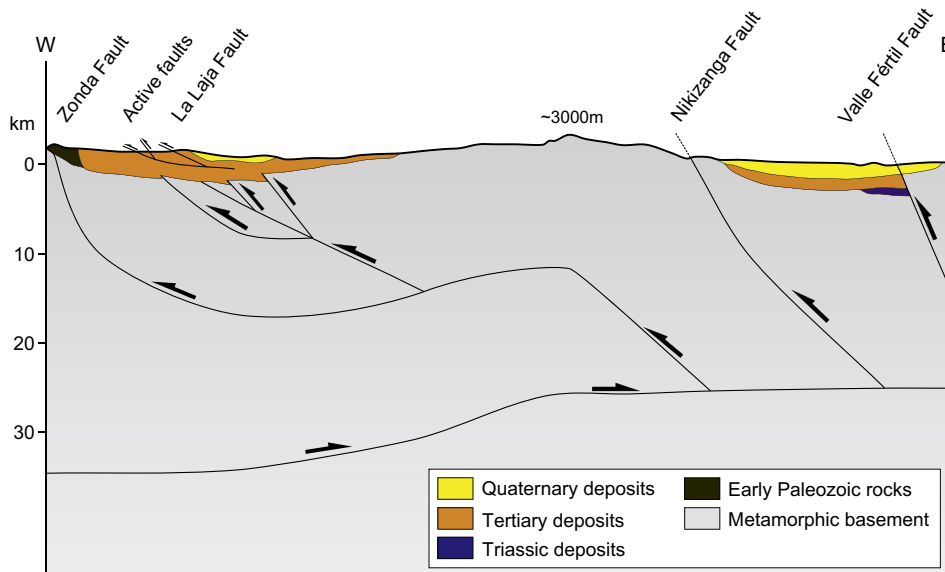


Fig. 2. The dominant structure of the crust beneath the Sierra de Pie de Palo is an east-vergent crustal basement wedge (modified from Ramos et al. (2002)).

Table 1
Zircon and apatite (U–Th)/He data of the samples from the Sierra de Pie de Palo.

Sample	Aliqu.	He		^{238}U		^{232}Th		Sm		Ejection correction (Ft)	Uncorr. [Ma]	Corr. [Ma]	2σ [Ma]	Mean age [Ma]	$\pm 2\sigma$ [Ma]
		Vol. [ncc]	1 σ [%]	Mass [ng]	1 σ [%]	Mass [ng]	1 σ [%]	Mass [ng]	1 σ [%]						
Zircon															
APM 09-09	z1	14.879	1.6	0.589	1.8	0.208	2.4	0.012	12	0.69	189.9	275.9	28.8	287.3	28.6
	z2	18.648	1.6	0.710	1.8	0.196	2.4	0.020	11	0.69	200.7	290.9	30.3		
	z3	34.307	1.6	1.278	1.8	0.350	2.4	0.109	12	0.73	205.0	281.8	26.5		
	z4	16.259	1.6	0.572	1.8	0.167	2.4	0.021	12	0.72	216.2	300.4	28.9		
APM 10-09	z1	21.470	1.6	0.868	1.8	0.604	2.4	0.359	7	0.76	172.9	226.5	19.1	252.4	17.3
	z2	98.612	1.6	3.066	1.8	0.242	2.4	0.060	8	0.86	255.6	298.5	19.1		
	z3	315.484	1.6	10.862	1.8	1.825	2.4	2.303	8	0.86	226.5	264.9	16.9		
	z4	264.292	1.6	11.226	1.8	0.575	2.4	2.813	8	0.86	189.1	219.7	13.9		
A 5-10z1	z1	221.648	1.6	7.845	1.8	1.841	2.4	0.207	10	0.84	217.5	259.7	17.5	278.8	19.1
	z3	248.267	1.6	7.600	1.8	2.321	2.4	0.126	10	0.83	247.0	298.0	20.6		
AUY 57-10	z4	12.767	1.7	0.447	1.9	0.153	2.4	0.013	11	0.71	214.9	303.2	30.1		
AUY 59-10	z5	12.252	1.7	0.403	1.9	0.133	2.4	0.018	11	0.70	229.1	325.9	32.8	303.2	33.2
	z6	13.845	1.7	0.492	1.8	0.088	2.4	0.010	14	0.71	219.2	309.2	30.7		
	z7	21.697	1.7	0.613	1.8	0.239	2.4	0.015	11	0.71	262.5	368.7	36.2		
Apatite															
A5-10	a1	0.044	5.5	0.003	29.1	0.007	3.9	0.611	7	0.87	38.4	43.9	9.4	46.1	9.3
	a4	0.056	5.2	0.004	20.8	0.003	5.1	0.851	7	0.84	40.4	48.3	9.3		
APM 09-09	a1	0.001	44.5	0.002	36.2	0.011	3.3	0.009	9	0.84	1.1	1.3	1.2	3.4	1.5
	a3	0.002	16.9	0.003	17.7	0.013	3.1	0.009	8	0.82	2.8	3.5	1.3		
	a4	0.003	13.3	0.002	30.2	0.012	3.3	0.011	9	0.88	4.8	5.4	2.0		
APM 10-09	a3	0.224	2.1	0.017	3.6	0.020	2.8	0.117	6	0.89	81.0	91.0	6.9	102.6	6.5
	a4	0.981	1.8	0.055	2.1	0.078	2.5	0.407	7	0.91	104.4	114.3	6.2		
AUY 56-10	a1	0.553	2.1	0.036	2.6	0.002	6.0	0.462	9	0.86	112.7	130.9	10.0	131.3	10.0
	a2	0.689	2.1	0.045	2.3	0.006	4.1	0.459	9	0.86	113.6	131.7	9.5		
	a3	0.529	2.3	0.035	2.5	0.002	5.9	0.331	9	0.86	112.4	131.4	10.3		
AUY 57-10	a1	No reliable data due to insufficient He-content													
	a2														
	a3														
AUY 59-10	a1	0.061	4.6	0.007	9.4	0.008	3.7	0.078	9	0.91	52.3	57.4	9.4	58.6	9.9
	a2	0.062	4.8	0.006	11.6	0.012	3.2	0.079	9	0.93	55.5	59.7	10.2		

Notes: aliqu. = aliquote, uncorr. = uncorrected age, and Ft-corr. = Ft-corrected age. Amount of helium is given in nano-cubic-cm in standard temperature and pressure; amount of radioactive elements are given in nanograms; ejection correct. (Ft): correction factor for alpha-ejection (according to Farley et al. (1996) and Hourigan et al. (2005)); uncertainties of helium and the radioactive element contents are given as 1 sigma, in relative error %; uncertainty of the single grain age is given as 2 sigma in Ma and it includes both the analytical uncertainty and the estimated uncertainty of the Ft; uncertainty of the sample average age is 2 standard error, as $(SD)/(n)^{1/2}$; where SD = standard deviation of the age replicates and n = number of age determinations. Four to six aliquots per sample were picked and analysed. If the investigated age of a single grain deviates by more than 2σ from the mean age, the aliquot was rejected. These erroneous ages can be caused by several factors, such as zoning of alpha-emitting elements, micro inclusions, the limit of detection, or the bias of the ejection correction (smaller grains have larger errors).

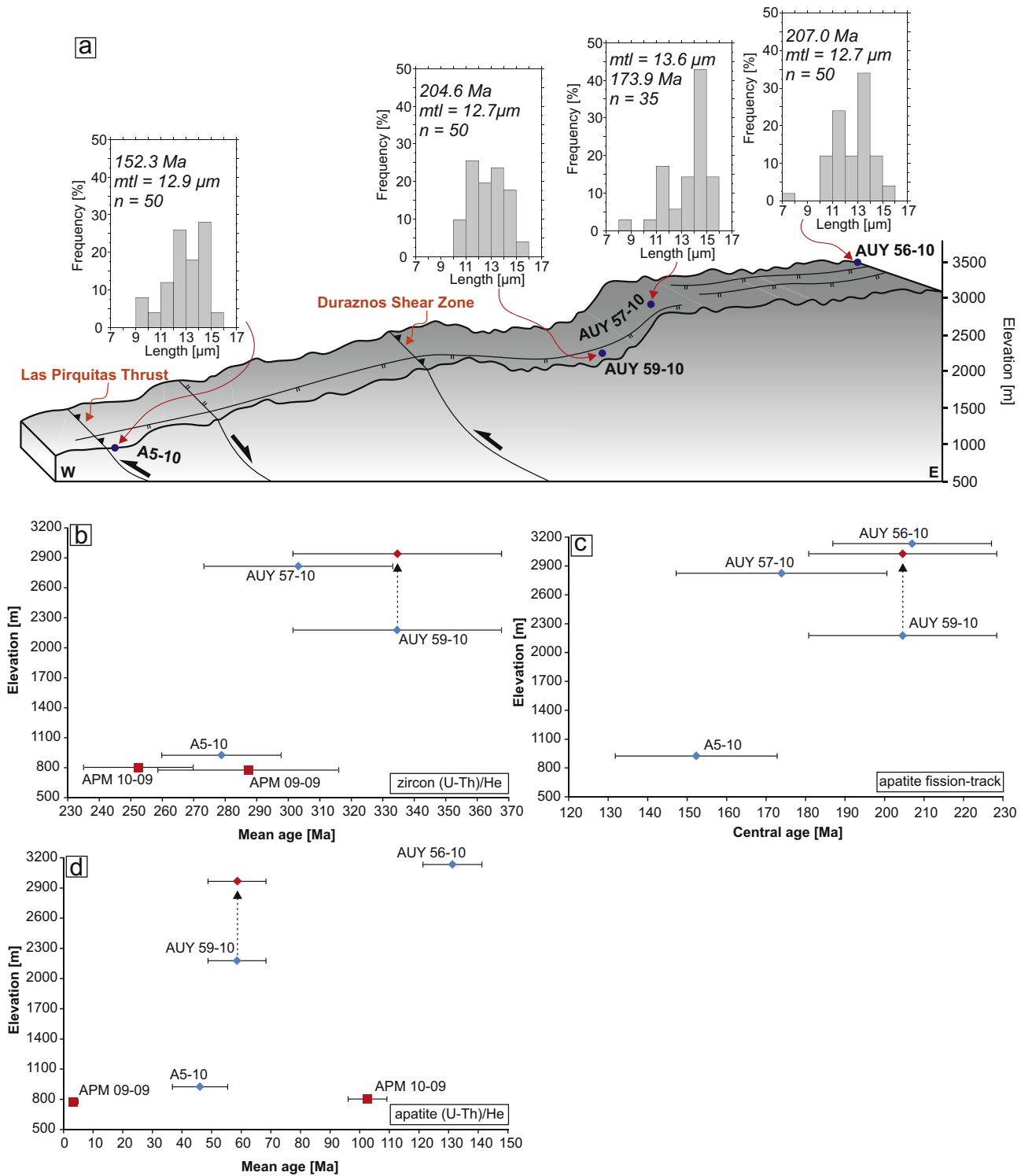


Fig. 3. Thermochronological results of the samples from the Sierra de Pie de Palo. a) Schematic profile across the mountain range along the investigated samples with the major structures (surface exposure of faults is just schematic). The apparent fission-track age, the corresponding track length distribution, the mean track length (mtl), and the number of confined tracks (n) measured for each sample are also shown. b), c) and d) Age-elevation plot for the ZHe-, AFT- and AHe-system, respectively. Samples, which are not collected along the profile are indicated by red squares in b) and d). Since AUY 59-10 is presumably relatively displaced to AUY 57-10 along a normal fault, the red point in b), c), and d) would be the approximated projected elevation of the former sample in an undisturbed profile. (For interpretation of the references to colour in this figure legend, the reader is referred to the web version of this article.)

during the Oligocene to Miocene and final flat-slab subduction-related exhumation (e.g. [Jordan et al., 1983](#); [Ramos et al., 2002](#); [Yáñez et al., 2001](#)) of the Pampean ranges commenced in Miocene-Pliocene times.

The aim of this study is to investigate the Cenozoic cooling exhumation and uplift ([England and Molnar, 1990](#)) history of the Sierra de Pie de Palo and its relationship to the Andean deformation within the Western Sierras Pampeanas using geochronological

Table 2

Apatite fission-track data of the samples from the elevation profile within the Sierra de Pie de Palo.

Sample (rocktype)	Longitude (W) latitude (S)	Elevation [m]	<i>n</i>	ρ_s	N_s	ρ_i	N_i	ρ_d	N_d	$P(X^2)$ [%]	Age [Ma]	$\pm 1\sigma$ [Ma]	MTL [μm]	s.d. [μm]	<i>N(L)</i>	Dpar [μm]	s.d. [μm]
A5-10 (gneiss)	68° 08' 36" 31° 22' 40"	925	25	3.34	221	2.10	139	6.00	5409	100	152.3	20.5	12.9	1.5	50	1.9	0.14
AUY 56-10 (mylonite)	67° 55' 46" 31° 18' 43"	3133	25	13.14	872	7.58	503	7.51	5725	99.1	207.0	20.1	12.7	1.4	50	1.9	0.09
AUY 57-10 (gneiss)	67° 58' 14" 31° 22' 30"	2824	25	2.13	164	1.16	89	5.92	5409	100	173.9	26.7	13.6	1.6	35	2.2	0.15
AUY 59-10 (gneiss)	67° 58' 56" 31° 23' 15"	2177	25	3.82	390	2.13	217	7.16	5409	96.7	204.6	23.8	12.7	1.3	50	1.9	0.13

Notes: *n*, number of dated apatite crystals; ρ_s/ρ_i , spontaneous/induced track densities ($\times 10^5$ tracks cm^{-2}); N_s/N_i , number of counted spontaneous/induced tracks; N_d , number of tracks counted on dosimeter; $P(X^2)$, probability obtaining chi-squared value (X^2) for *n* degree of freedom (where *n* is the number of crystals – 1); age $\pm 1\sigma$ is central age ± 1 standard error (Galbraith and Laslett, 1993); ages were calculated using zeta calibration method (Hurford and Green, 1983); glass dosimeter CN-5, and zeta value of 323.2 ± 25.3 ; MTL, mean track length; s.d., standard deviation of track length distribution and Dpar measurements; *N*, number of tracks measured; Dpar, etch pit diameter.

methods. Therefore, we conducted apatite fission-track measurements, (U–Th)/He analysis of zircon and apatite of samples from the Sierra de Pie de Palo, and subsequent thermal modelling to get complete cooling paths from below approximately 200 °C to surface temperature.

2. Geologic setting

The Sierra de Pie de Palo located between 67°30'–68°30' W and 31°00'–32°00' S is one of the westernmost ranges of the Argentine Sierras Pampeanas (Fig. 1). It represents a NNE trending elongated dome with an area of approximately 2400 km² and elevations of more than 3000 m. This fault bounded basement anticline (Perez and Martínez, 1990) is part of the Western Sierras Pampeanas (sensu Caminos, 1979; Pankhurst and Rapela, 1998) constituting the central part of a N–S trending belt, the Cuyania Terrane (Sato et al., 2000), which accreted along a major suture west of the Valle Fértil (e.g. Ramos et al., 2002) to the southwestern proto-Andean margin of Gondwana during the Late Paleozoic (e.g. Ramos, 1988; Keller et al., 1998; Pankhurst and Rapela, 1998; Ramos et al., 1998; Ramos, 2004; Rapela et al., 1998; Thomas and Astini, 2003). Beside the Sierra de Pie de Palo, further morphological features farther to the north and south within this belt are the Sierra Toro Negro, Sierra Umango, Sierra Maz, and Sierra Espinal as well as the San Rafael and Las Matras blocks, respectively (e.g. Sato et al., 2000, 2004; Ramos, 2004). Overall, these mountain ranges are mainly composed of Mesoproterozoic to Early Paleozoic rocks, which are considered being the basement of the Cuyania Terrane (Astini et al., 1995; Casquet et al., 2001; Sato et al., 2000, 2004).

Within the Sierra de Pie de Palo the basement is characterised by a nappe structure (e.g. Bollinger and Langer, 1988; Meira et al., 2012; Vujovich et al., 2004), which is related to an E–W compression and an orthogonal collision during the Famatinian orogenic cycle (e.g. Le Corre and Rossello, 1994; Martino, 2003; Simpson et al., 2003; van Staal et al., 2011). Additionally, this deformation-regime caused a top-to-the-west vergence expressed in the basement units and by the Early Paleozoic N–S trending thrust systems, e.g. the Las Pirquitas Thrust, controlling the contact between the different metamorphic sequences within the mountain range (Fig. 1b; Dalla Salda and Varela, 1984; Ramos et al., 1998; Ramos and Vujovich, 2000). These units are represented by *i*) the Neoproterozoic to Cambrian Caucete Group (e.g. Casquet et al., 2001; Naipauer et al., 2010; Ramos et al., 1996), consisting of metasedimentary sequences, i.e. low- to medium-grade quartzite and marble (e.g. Naipauer et al., 2010; Vujovich, 2003), which is assumed to be an equivalent of the Cambrian platform sequence of the Precordillera (Galindo et al., 2004; Naipauer et al., 2010; Ramos et al., 1998; Vujovich and Kay, 1998); *ii*) the Mesoproterozoic Pie de Palo Complex (e.g. Dalla Salda and Varela, 1984; Ramos et al., 1998;

Ramos and Vujovich, 2000; Vujovich and Kay, 1998), juxtaposed with the Caucete Group along the Las Pirquitas Thrust (Ramos et al., 1996), consists of ultramafic to mafic rocks and amphibolites in the area between the Las Pirquitas Thrust and the Duraznos Shear Zone (Fig. 1b), intermediate orthogneisses and qtz-fsp-ms-ep shists east of the Duraznos Shear Zone (Fig. 1b), and orthogneisses as well as shists in the eastern area of the Sierra de Pie de Palo (Fig. 1b; e.g. Ramos et al., 1998; Ramos and Vujovich, 2000; Varela et al., 2011); *iii*) the Difunta Correa Metasedimentary Sequence (Fig. 1b; Baldo et al., 1998), mainly composed of Ca-pelitic shists, quartzites, marbles, and less abundant amphibolites (Baldo et al., 1998), is considered being the Neoproterozoic sedimentary cover of the Pie de Palo Complex (Galindo et al., 2004); and *iv*) the Neoproterozoic Quebrada Derecha Orthogneiss described in detail by (Baldo et al., 2006).

Accretion and deformation in the Early Paleozoic was followed by orogenic collapse during the Late Paleozoic (Mpodozis and Ramos, 1989) leading to extensional reactivation of the former major sutures and the formation of the Paganzo Basin (e.g. Ramos et al., 2002). Main depocentres of this basin are associated and controlled by the crustal discontinuities inherited from the Early Paleozoic deformation (Fernandez Sevesco et al., 1993; Ramos et al., 2002). One of these depocentres is west of the Valle Fértil Fault containing Carboniferous deposits separating the Sierra de Pie de Palo from the mountain ranges further to the east (Ramos et al., 2002; Regnier et al., 1992). Sedimentary successions deposited on these Carboniferous sediments are mainly related to Mesozoic rifting and Andean compression in the Cenozoic (e.g. Ramos et al., 2002). During the latter the Mesozoic normal faults were inversely reactivated resulting in a diachronous uplift of the Sierras Pampeanas and uplift of the Precordillera (e.g. Jordan and Allmendinger, 1986; Jordan et al., 1989). According to Ramos and Vujovich (2000) synorogenic sediments derived from the latter covered the Sierra de Pie de Palo in the Late Pliocene.

Uplift and exhumation accompanied by deformation of the Sierra de Pie de Palo commenced at approximately 3 Ma and still continues showing an uplift rate of 1 mm/a and a shortening rate of 4 mm/a (Ramos and Vujovich, 2000; Ramos et al., 2002). According to the authors these processes are controlled by a mid-crustal basement wedge (Fig. 2), whereas (Vita-Finzi, 2009) interprets the Sierra de Pie de Palo representing a cataclastic diapir, which is primarily uplifted and exhumed by lateral compressive forces and secondarily by density differences.

3. Thermochronological methods

The combination of different temperature-dependent geochronometers, e.g. (U–Th)/He of zircon and apatite as well as apatite fission-track, is a suitable approach to reconstruct

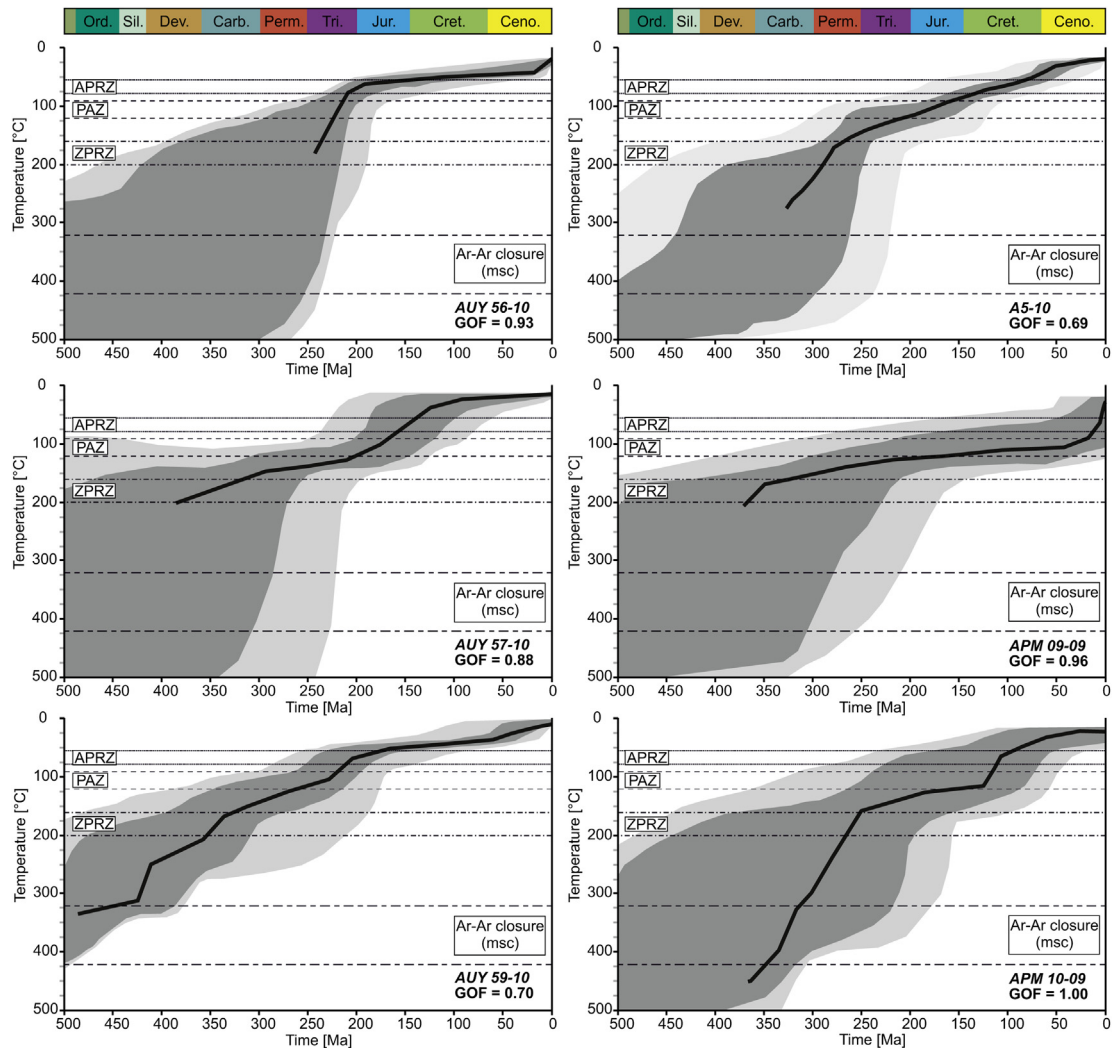


Fig. 4. Time-temperature history derived by thermal modeling including the ranges of the effective closure temperatures for the different dating systems, where APRZ/ZPRZ represents the partial retention zone of apatite/zircon (called PR_Z/PR_Z in the text), PAZ defines the partial annealing zone, and GOF the goodness of fit between the measured and modelled data averaged for all considered systems. The black curve indicates the average fit, good fits are shown in dark grey, and acceptable fits in light grey. Note that the individual average fits do not necessarily represent the overall cooling/exhumation path of the mountain range, meaning that the general cooling path could also lie within the range of good and acceptable fits of the individual samples. The starting constraint set (muscovite Ar–Ar closure temperature and related age obtained by Mulcahy et al. (2011) is also shown, but not to scale. Ord. = Ordovician, Sil. = Silurian, Dev. = Devonian, Carb. = Carboniferous, Perm. = Permian, Tri. = Triassic, Jur. = Jurassic, Cret. = Cretaceous, Cen. = Cenozoic.

temperature-age relationships below 200 °C, thus the cooling/exhumation history of mountain ranges (e.g. Farley et al., 1996). These geochronological systems are thermally sensitive over geological times for temperature intervals, namely the partial retention zone (PR_{Z/A}) for the zircon and apatite (U–Th)/He system (ZHe and AHe, respectively; e.g. Baldwin and Lister, 1998; Wolf et al., 1998) and the partial annealing zone (PAZ_A) for the apatite fission-track system (AFT; e.g. Gleadow and Fitzgerald, 1987). Depending on the retentivity of radiogenic helium within the zircon and apatite crystals and the fission-tracks in the apatite crystals these intervals range between 200–160 °C, 80–55 °C, and 120–90 °C for the PRZ of zircon and apatite as well as the PAZ_A, respectively (e.g. Laslett et al., 1987; Donelick et al., 1999; Farley, 2000; Reiners et al., 2004). In turn, the retention behaviour of the radiogenic helium in the (U–Th)/He system and of the fission-tracks in the AFT system is mainly controlled by grain size, crystal morphology, alpha-damage density, and cooling rate (e.g. Wolf et al., 1996; Ehlers and Farley, 2003; Reiners and Brandon, 2006) as well as by cooling rate and kinetic parameter of track annealing,

which is described by the etch pit diameter (Dpar) roughly representing an indication of the chemical composition (Donelick et al., 1999; Ketcham et al., 1999; Reiners and Brandon, 2006), respectively.

During this study, basement samples from an elevation profile in the Sierra de Pie de Palo as well as two samples from the western margin and the southern tip of the mountain range, respectively (Fig. 1a), were investigated using the AHe and ZHe method. Additionally, apatite fission-track dating was applied on the samples from the elevation profile (Fig. 1a). The sample treatment and preparation procedure are described in more detail by (Löbens et al., 2011).

4. Results

4.1. Zircon (U–Th)/He

Mean zircon helium ages range from 334 Ma (Carboniferous) to 252 Ma (Permian–Triassic). Three samples were taken along the

elevation profile (A5-10, AUY 59-10, AUY 57-10). In general, the obtained ages correlate with elevation, showing youngest ages in lower elevated areas and increasing ages towards higher altitudes (Table 1, Fig. 3). Due to an insufficient amount of suitable zircon crystals, no age could be obtained from the topmost sample (AUY 56-10). The samples APM 09-09 and APM 10-09, which both represent amphibolite, from the western margin and the southern tip of the mountain range, respectively, yield ages of 287.3 ± 28.6 Ma (APM 09-09) and 252.4 ± 17.3 Ma (APM 10-09, Table 1, Fig. 3b).

4.2. Apatite fission-track

Central ages of the samples from the elevation profile within the Sierra de Pie de Palo (Fig. 1a) range between the Late Triassic and the Late Jurassic (Fig. 3, Table 2). There is a distinct correlation between age and elevation (Fig. 3) with an age of 207.0 ± 20.1 Ma (AUY 56-10) and 152.3 ± 20.5 Ma (A5-10) at the top and the bottom of the range, respectively (Fig. 3a). An exception of this trend is represented by sample AUY 57-10, which is situated at a relatively greater elevation than AUY 59-10 but is younger (173.9 ± 26.7 Ma) than the latter (204.6 ± 23.8 Ma, Fig. 3a, c, Table 2).

All samples are characterised by distinct shortened tracks (Fig. 3a). The mean track length varies from 12.68 ± 1.44 μm (AUY 56-10) to 13.57 ± 1.63 μm (AUY 57-10). For samples A5-10, AUY 56-10, and AUY 57-10 these lengths are bimodal distributed (Fig. 3a), but for A5-10 less distinct than for the latter two. Contrastingly, AUY 59-10 yields an unimodal track length distribution (Fig. 3a). The mean etch pit diameter of the four investigated samples ranges between 1.88 ± 0.09 μm and 2.24 ± 0.15 μm (Table 2).

4.3. Apatite (U–Th)/He

The unweighted average ages of the five analysed samples from the Sierra de Pie de Palo range between the Early Cretaceous and the Pliocene (Table 1). Samples A5-10, AUY 56-10, and AUY 59-10, situated along the elevation profile (Fig. 1a), show a distinct positive correlation between age and elevation (Fig. 3d). The lowest and the topmost samples (A5-10 and AUY 56-10) yield ages of 46.1 ± 9.3 Ma and 131.3 ± 9.96 Ma, respectively (Table 1). APM 10-09, located at the southern tip of the mountain range, shows an age of 102.7 ± 6.5 Ma and APM 09-09 from the western margin of the range yields an age of 3.4 ± 1.5 Ma (Fig. 3d, Table 1).

5. Discussion

5.1. Thermal modelling

The thermal history of six samples from the Sierra de Pie de Palo was modelled using the HeFTy software (Fig. 4; Ketcham, 2005). The input data for the modelling were the fission-track single grain ages, track length distribution, and Dpar data, as well as the corresponding apparent zircon and apatite (U–Th)/He ages. If all single grain ages of a sample show unusual ages concerning the U–Th/He system, i.e. AHe ages of AUY 57-10, which is probably related to small inclusions or to an insufficient He content, the affected system was not considered by thermal modelling. The starting- and end-point of the modelled time-temperature history were constrained by Ar–Ar data of muscovite (closure temperature of approx. 400 °C) reported by Mulcahy et al. (2011) and the mean annual surface temperature of 17 °C (Müller, 1996), respectively. Further constraints set are related to the measured ages of the different systems.

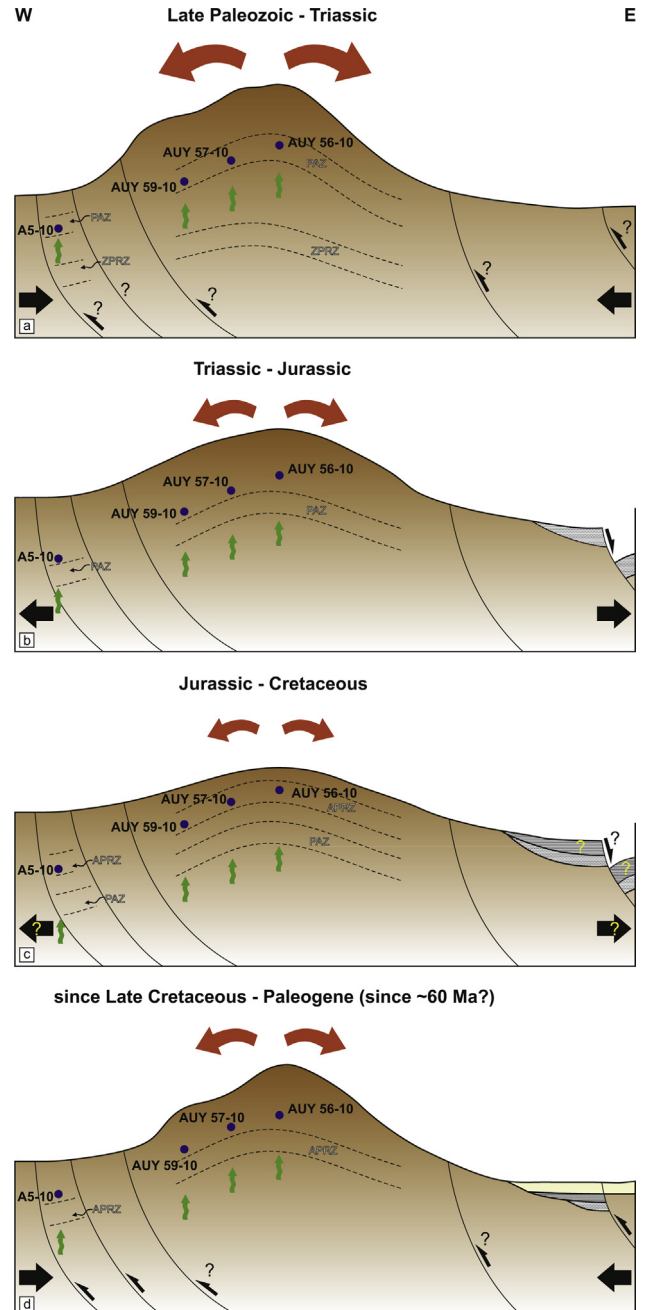


Fig. 5. Schematic sketch of the structural evolution of the Sierra de Pie de Palo through time (vertical exaggerated) based on the new thermochronological data and the modelled time-temperature history. APRZ/ZPRZ = partial retention zone of apatite/zircon, PAZ = partial annealing zone, red arrows = relative mass and direction of erosionally removed material, green arrows = exhumation, bold black arrows = tectonic regime, black and yellow question marks = uncertainties about sedimentary sequence/tectonic regime and fault activity as well as its timing. Note that possible advection of isotherms is not considered. Further details are in the text. (For interpretation of the references to colour in this figure legend, the reader is referred to the web version of this article.)

5.2. General structural evolution of the Sierra de Pie de Palo

The modelled time-temperature histories suggest that general cooling below ~ 175 °C commenced between the Late Paleozoic (Fig. 4). This cooling, hence exhumation is probably related to erosion affecting the rugged relief generated during the Famatinian Orogeny, which is associated with accretion of the Cuyania Terrane at the southwestern proto-Andean margin of Gondwana during the

Paleozoic (Fig. 5a, e, g. Pankhurst and Rapela, 1998). Potentially, further exhumation of our samples from the PRZ_Z into the PAZ_A (Figs. 4 and 5a) during Permian and Triassic times was caused by a Permo-Triassic compressional phase described by Ramos and Folguera (2009) among others and the related tectonically triggered erosion (Fig. 5a).

Although the inflection point for the AFT thermochronometer (Fig. 3c) is not well constrained the modelled cooling paths suggest that cooling below the lower thermal boundary of the PAZ_A occurred between the Late Triassic and the Jurassic (Fig. 4), possibly at around 170 Ma (Fig. 3c). This exhumation is presumably related to erosion controlled by extension, at least during the Triassic (e.g. Ramos et al., 2002). Associated Triassic rifting occurred along reactivated Paleozoic suture zones, i.e. the master fault bounding the Sierra de Valle Fértil in the west. Since the area of the Sierra de Pie de Palo was *i*) still characterised by a positive topography and *ii*) situated on the footwall, erosion, which probably mainly occurred towards the east, caused the cooling and exhumation (Figs. 4 and 5b). Subsequent cooling into the PRZ_A generally commenced during the Jurassic (Fig. 4). Since the area of the Sierra de Pie de Palo was presumably still characterised by a positive relief during that time, continuous erosion lead to exhumation of our samples to a temperature of approximately 65 °C (Figs. 4 and 5c). Additionally, sub-humid conditions during that time, as described by Carignano et al. (1999), would facilitate enduring erosion. Variations of individual cooling paths from this general trend (Fig. 4) are referred to the fault-related internal structure of the mountain range.

However, final cooling below the lower temperature boundary of the PRZ_A, thus exhumation towards the surface generally commenced between the Cretaceous and the Paleogene (Fig. 4); possibly, although not well constrained, at around 60 Ma (Fig. 3d). Exhumation due to erosion within the Sierra de Pie de Palo during the time of Cretaceous rifting, which was generated by the opening of the South Atlantic during that time (e.g. Schmidt et al., 1995), cannot completely be excluded. But since Cretaceous deposits are generally absent in the adjacent intracontinental basins (e.g. Zapata, 1998) and this extension rather affected the eastern part of the Sierras Pampeanas than the western part (e.g. Rosello and Mozetic, 1999; Ramos et al., 2002), it is not very likely that cooling of our samples is referred to this event. Furthermore, en-block uplift triggered by the ca. E–W compression during the early stage of the Andean deformation, which generated movement along the right lateral transpressional Tucumán Transfer Zone (TTZ; e.g. de Urreiztieta et al., 1996; Roy et al., 2006) and caused uplift of the early Puna Plateau further to the north (e.g. Carrapa et al., 2005; Löbens et al., 2013) can rather be excluded since the length distributions of the fission-tracks do not indicate a fast exhumation being characteristic for tectonically related exhumation (Fig. 3a). Therefore, and due to the thermal models (Fig. 4), which indicate a continuous cooling, exhumation in the area of the Sierra de Pie de Palo is most likely generated by erosion of a positive topography (see below; Fig. 5d).

However, based on our interpretations of the obtained thermal models two different hypotheses concerning the Cenozoic structural and thermal evolution of the Sierra de Pie de Palo can be considered; *i*) a positive relief since the Paleocene; possibly since ~60 Ma as indicated by the age-elevation relationship (Fig. 3d); and *ii*) an area acting as accommodation space for Pliocene sediments derived from the Precordillera before being uplifted in post-Pliocene times.

- i) Due to the thermal modelling suggests continuous exhumation within the Sierra de Pie de Palo at least since the Late Mesozoic to Early Cenozoic, the area already had to be characterised by a positive relief (Fig. 5d). Furthermore, the region could still be

capped by a thin sedimentary cover, from that time until today (see below). If there would have been a flat topography and the area of the recent mountain range was entirely covered by a substantial amount of Pliocene sediments derived from the uplifted Precordillera until 3 Ma as proposed by Ramos et al. (2002), the time-temperature paths should indicate a re-heating or at least stagnation in cooling caused by burial beneath these deposits rather than cooling (Fig. 4). Therefore, we propose that there had to be some kind of topography in the vicinity of the Sierra de Pie de Palo before 3 Ma, otherwise there would not have been any erosion causing cooling/exhumation of our samples since the Late Cretaceous to Paleogene, as indicated by modelled t-T-paths (Figs. 4 and 5d). Further, although our data and the related models do not illuminate the amount of uplift generated by the Andean deformation which is additionally characterised by the flat-slab subduction in the Late Cenozoic, uplift presumably was less than the 3 km (present elevation) in the last 3 Ma as suggested by Ramos et al. (2002) because of the positive relief controlling continuous exhumation as mentioned above.

- ii) Alternatively, exhumation below the PRZ_A was caused by erosion from the Late Cretaceous to the Late Miocene eliminating any topography and producing accommodation space in the Pie de Palo region filled by sediments derived from the Precordillera during the Pliocene (Ramos et al., 2002). Subsequently, continuous Andean deformation uplifts the Sierra de Pie de Palo to a present-day peak elevation of 3 km in the last 3 Ma (Ramos et al., 2002). Therefore, exhumation had to be more than 3 km because of the sedimentary Pliocene cover. Further, the thermal models do not suggest re-heating (Fig. 4), thus thickness of these sediments could be limited by the temperature of the PRZ_A. If the sedimentary thickness would cause burial re-heating to temperatures above the lower PRZ_A temperature, any age reset should be visible in the mean AHe ages. But since Tertiary deposits are up to 10 km thick in the Bermejo Basin east of the Sierra de Pie de Palo (Zapata, 1998), it is doubtful that there was no substantial sedimentary cover atop of the range, which would have caused re-heating at least to temperatures characteristic for the PRZ_A during the Cenozoic. Additionally, any sedimentation scenario contradicts this continuous exhumation since at least the Mesozoic as indicated by the time-temperature relationship (Fig. 4).

Therefore, based on our data this Cenozoic evolution is rather questionable and we favour the first hypothesis, which does not completely exclude exhumation and uplift caused by the flat-slab subduction during the Middle to Late Pliocene as indicated by deformed Pliocene sediments on the eastern and western flanks of the Sierra de Pie de Palo (Ramos and Vujovich, 2000). Furthermore, this interpretation does also not argue against deformed lacustrine sections within these Pliocene sediments (Ramos and Vujovich, 2000). Presumably, these units were deposited in local depressions representing playa-lake environments at the flanks of the elevated area during the Early Pliocene and were deformed in the Middle to Late Pliocene. This recorded deformation could possibly contribute to the exhumation and uplift of the Sierra de Pie de Palo, but just to minor extend. As mentioned above, the amount of Pliocene to post-Pliocene uplift was presumably less than the 3 km proposed by Ramos et al. (2002), hence these deformational processes just accentuated the existing relief.

5.3. Internal structure and related exhumation

The internal structure of the Sierra de Pie de Palo is mainly controlled by Paleozoic N–S trending thrusts, e.g. the Las Pirquitas

Thrust and the Duraznos Shear Zone, and ~E–W striking normal faults (Figs. 1b and 3a). These ~E–W trending normal faults dominantly affect local differences in the thermochronological ages, especially the apatite fission-track ages (Fig. 3). Concerning this system the cross-section is disturbed by normal faulting between samples AUY 57-10 and AUY 59-10, as suggested by the geological map of the Sierra de Pie de Palo (Fig. 1b; Ramos and Vujovich, 2000), resulting in an older central age of the relatively lower sample AUY 59-10 (Fig. 3). Basing on the AFT ages a re-projection would lead this sample formerly being at an elevation between samples AUY 56-10 and AUY 57-10, hence between 3133 m (recent crestal elevation) and 2824 m, respectively (Fig. 3). But due to the apatite fission-track ages (central age and observed single grain ages) of AUY 59-10 are similar to those of AUY 56-10, initial elevation of the former presumably was closer to 3133 m than to 2824 m. Further, this re-projection results in *i*) a better constraint of the potential inflection point, which seems to be around 172 Ma (Fig. 3) and *ii*) in a maximal displacement of approximately 956 m (difference between the present elevation of AUY 59-10 and 3133 m) along the E-W trending normal fault affecting the investigated profile (Figs. 1b and 3). Since this fault probably also generated a displacement of sample A5-10 as suggested by its trace (Figs. 1b and 3) the latter also has to be re-projected by a maximum offset of 956 m resulting in an initial elevation of around 1881 m. Therefore, A5-10 is still relatively lower than AUY 57-10, thus the maximal offset is plausible. Furthermore, a time constraint of fault activity is just suggested by the AHe data. Since there is no fault-related disturbance of the AHe ages in the cross-section, movement along the normal fault probably occurred before 60 Ma, indicated by the possible, but not well constrained, inflection point (Fig. 3d). Although there is no AHe data of sample AUY 57-10 which would confirm this hypothesis, we propose that the significantly younger age of AUY 59-10 compared to AUY 56-10 implies an undisturbed profile regarding this certain fault since around 60 Ma. Otherwise, if faulting would also perturb the AHe ages within the profile, the age of AUY 59-10 probably would have been similar to that of AUY 56-10 like in the AFT system (Fig. 3).

However, although the two other basement samples lack AFT-data their cooling histories also suggest continuous exhumation at least since the Mesozoic (Fig. 4). Furthermore, exhumation occurred earlier in the eastern part of the mountain range (Figs. 1 and 4, APM 10-09) than at the western margin (APM 09-09), where it is presumably related to Neogene movement along the Las Pirquitas Thrust (Figs. 1b, 3a and 4, Table 1). Therefore, deformation and exhumation probably propagated towards the west as also proposed by Coughlin et al. (1998) for at least the Sierra Famatina. But these authors restrict westward propagation to Miocene-Pliocene times, whereas our data suggest that deformation in the most eastern area of the Sierra de Pie de Palo already occurred in the Late Mesozoic. Therefore, final cooling and exhumation of the region below the lower temperature boundary of the PRZ_A is presumably closely related to commencement of movement along the TTZ during the Late Mesozoic-Cenozoic induced by the Andean deformation (e.g. de Urreiztieta et al., 1996; Roy et al., 2006).

5.4. Cenozoic thermal evolution and amount of exhumation in the Sierra de Pie de Palo

Since a perturbation of the geothermal gradient by advection through volcanic activity can be excluded in the area of the Sierra de Pie de Palo during the Early Cenozoic, an extrapolation of 20–26 °C/km assumed by Sobel and Strecker (2003) and Löbens et al. (2013) for the Northern Sierras Pampeanas and by Löbens et al. (2011) for the Eastern Sierras Pampeanas to the Western Sierras Pampeanas is suitable. Based on this geothermal gradient and assuming an

effective closure temperature (T_C) of around 60 °C for the AHe-system as well as a paleo-surface temperature of 17 °C, there had to be an exhumation between 2.2 km (20 °C/km) and 1.7 km (26 °C/km) during the Cenozoic bringing samples to the surface. Therefore, average exhumation rate, which is mainly controlled by erosion, would be around 0.04–0.03 mm/a since 60 Ma, when cooling below approximately 60 °C occurred (Figs. 4 and 5d). Further, since the adjacent Bermejo Basin is characterised by 5–10 km thick Tertiary deposits (Zapata, 1998) a rock column of up to ~2 km above our samples, which had to be eroded since 60 Ma in order to allow this exhumation, is plausible. Furthermore, since the top sample (AUY 56-10) is at an elevation of 3 km today vertical rock uplift had to be between 3.7 km and 4.2 km during the Cenozoic.

However, if the Sierra de Pie de Palo was completely covered by Pliocene deposits as proposed by Ramos and Vujovich (2000) and Ramos et al. (2002), these sediments could not be thicker than approximately 3 km (as mentioned above), which is equivalent to 60 °C for a geothermal gradient of 20 °C/km, because the modelled cooling path do not indicate a re-heating/burial in the Late Cenozoic (Fig. 4). Therefore, the maximum exhumation rate would be around 1 mm/a being equivalent to the surface uplift rate proposed by Ramos et al. (2002). But since there is rather a continuous exhumation for the whole Cenozoic, as suggested by the modelled time-temperature histories (Fig. 4) and as mentioned above, than an increase of the exhumation rate in the Late Cenozoic, the hypothesis that uplift of peak level commenced in the Pliocene is arguable. Instead, this process was presumably generated earlier, possibly also between the Late Cretaceous and Paleocene, otherwise there could not have been continuous erosion, thus exhumation, as suggested by the time-temperature histories (Fig. 4). But our data do not illuminate the onset more precisely.

6. Conclusions

- 1) Cooling and exhumation below ca. 175 °C in the Sierra de Pie de Palo is mainly controlled by erosion affecting a rugged relief generated during the Famatinian Orogeny.
- 2) Exhumation of our samples from the PRZ_Z into the PAZ_A occurred during Permian and Triassic times and is related to erosion controlled by a Permo-Triassic compressional phase.
- 3) During the Mesozoic further cooling and exhumation in the area of the Sierra de Pie de Palo is related to erosion affecting a positive relief being occasionally controlled by an extensional tectonic setting.
- 4) Final cooling and exhumation of the Sierra de Pie de Palo commenced between the Cretaceous and the Paleogene, possibly at around 60 Ma, being related to erosion of an existing positive topography.
- 5) Westward propagation of deformation and exhumation in the Western Sierras Pampeanas, at least in the Sierra de Pie de Palo, has probably been occurred since the Late Mesozoic to Paleogene.
- 6) Overall 3.7–4.2 km vertical rock uplift occurred in the Sierra de Pie de Palo since ~60 Ma, and the exhumation was between 2.2 km and 1.7 km resulting in an average exhumation rate of 0.04–0.03 mm/a since that time.
- 7) Peak level uplift of the Sierra de Pie de Palo probably also commenced at around 60 Ma in order to allow continuous erosion since that time; thus Pliocene surface uplift, previously assumed being around 3 km, is presumably overestimated.

Acknowledgements

This research project was financed by the German Research Council (DFG project SI 438/31-1). We are grateful for help of Carlos

H. Costa, Emilio Ahumada, and Mónica López de Luchi alleviating the stay in Argentina, as well as André Steenken and Juan Antonio Palavecino assisting during the field-work.

References

- Aceñolaza, F.G., Toselli, A.J., 1988. El Sistema de Famatina, Argentina: su interpretación como orógeno de margen continental activo. In: V Congreso Geológico Chileno, vol. 1, pp. 55–67.
- Astini, R.A., Benedetto, J.L., Vaccari, N.E., 1995. The early Paleozoic evolution of the Argentine Precordillera as a Laurentian rifted, drifted, and collided terrane: a geodynamic model. *Geol. Soc. Am. Bull.* 107 (3), 253–273.
- Baldí, B.A., Peralta, S.H., Villegas, R., 1989. Esquematizaciones de una posible transcurrida del terrane de Precordillera como fragmento continental procedente de áreas pampeano-bonaerenses. *Correlaciones Geol. Univer. Nacional Tucumán* 5, 81–100.
- Baldo, E., Casquet, C., Pankhurst, R., Galindo, C., Rapela, C., Fanning, C., Dahlquist, J., Murra, J., 2006. Neoproterozoic A-type magmatism in the Western Sierras Pampeanas (Argentina): evidence for Rodinia break-up along a proto-Iapetus rift? *Terra Nova* 18 (6), 388–394.
- Baldo, E.G., Casquet, C., Galindo, C., 1998. Datos preliminares sobre el metamorfismo de la Sierra de Pie de Palo, Sierras Pampeanas Occidentales (Argentina). *Geogaceta* 24, 39–42.
- Baldwin, S.I., Lister, G.S., 1998. Thermochronology of the south Cyclades shear zone, Ios, Greece: Effects of ductile shear in the argon partial retention zone. *J. Geophys. Res.* 103 (B4), 7315–7336.
- Bollinger, G.A., Langer, C.J., 1988. Development of a velocity model for locating aftershocks in the Sierra Pie de Palo region of western Argentina. *Bull. U.S. Geol. Surv.* Denver, 16.
- Caminos, R., 1979. Sierras pampeanas noroccidentales; Salta, Tucumán, Catamarca, La Rioja y San Juan. Córdoba, 225–291.
- Carignano, C., Cioccale, M., Rabassa, J., 1999. Landscape antiquity of the Central Eastern Sierras Pampeanas (Argentina): Geomorphological evolution since Gondwanic times. Berlin-Stuttgart: *Zeitschrift für Geomorphologie*, N.F., Supplement Band 118, 245–268.
- Carrapa, B., Adelmann, G., Hillyer, G.E., Mortimer, E., Sobel, E.R., Strecker, M.R., 2005. Oligocene range uplift and development of plateau morphology in the southern central Andes. *Tectonics* 24 (4). <http://dx.doi.org/10.1029/2004TC001762>.
- Casquet, C., Baldo, E., Pankhurst, R., Rapela, C., Galindo, C., Fanning, C., Saavedra, J., 2001. Involvement of the Argentine Precordillera terrane in the Famatinian mobile belt: U-Pb SHRIMP and metamorphic evidence from the Sierra de Pie de Palo. *Geology* 29 (8), 703.
- Coughlin, T.J., O'Sullivan, P.B., Kohn, B.P., Holcombe, R.J., 1998. Apatite fission-track thermochronology of the Sierras Pampeanas, central western Argentina: implications for the mechanism of plateau uplift in the Andes. *Geology* 26 (11), 999–1002.
- Dalla Salda, L., Varela, R., 1984. El metamorfismo en el tercio sur de la sierra Pie de Palo, San Juan. *Rev. Asoc. Geol. Argentina* 39 (1–2), 68–93.
- de Urreiztieta, M., Gapais, D., Le Corre, C., Cobbold, P.R., Rossello, E., 1996. Cenozoic dextral transpression and basin development at the southern edge of the Puna Plateau, northwestern Argentina. *Tectonophysics* 254 (1–2), 17–39.
- Donelick, R.A., Ketcham, R.A., Carlson, W.D., 1999. Variability of apatite fission-track annealing kinetics; II, crystallographic orientation effects. *Am. Mineral.* 84 (9), 1224–1234.
- Ehlers, T.A., Farley, K.A., 2003. Apatite (U–Th)/He thermochronometry: methods and applications to problems in tectonic and surface processes. *Earth Planet. Sci. Letters* 206 (1–2), 1–14.
- England, P., Molnar, P., 1990. Surface uplift, uplift of rocks, and exhumation of rocks. *Geology* 18 (12), 1173–1177.
- Farley, K.A., 2000. Helium diffusion from apatite: general behavior as illustrated by Durango fluorapatite. *J. Geophys. Res.* 105 (B2), 2903–2914.
- Farley, K.A., 2002. (U–Th)/He dating: techniques, calibrations, and applications. *Rev. Mineral. Geochem.* 47 (1), 819–844.
- Farley, K.A., Wolf, R., Silver, L., 1996. The effects of long alpha-stopping distances on (U–Th)/He ages. *Geochim Cosmochim Acta* 60 (21), 4223–4229.
- Fernandez Sevesco, F., Perez, M.A., Brisson, I.E., Alvarez, L.A., 1993. Sequence stratigraphy and tectonic analysis of the Paganza Basin, western Argentina. Buenos Aires. In: *Comptes Rendus XII ICC-p*, vol. 2, pp. 223–260.
- Finney, S., Gleason, J., Gehrels, G., Peralta, S., Aceñolaza, G., 2003. Early Gondwanan connection for the Argentine Precordillera terrane. *Earth Planet. Sci. Letters* 205 (3–4), 349–359.
- Fitzgerald, P., Baldwin, S., Webb, L., O'Sullivan, P., 2006. Interpretation of (U–Th)/He single grain ages from slowly cooled crustal terranes: a case study from the Transantarctic Mountains of southern Victoria Land. *Chem. Geol.* 225 (1–2), 91–120.
- Galbraith, R.F., Laslett, G.M., 1993. Statistical models for mixed fission track ages. *Nucl. Tracks Radiat. Meas.* 21 (4), 459–470.
- Galindo, C., Casquet, C., Rapela, C., Pankhurst, R., Baldo, E., Saavedra, J., 2004. Sr, C and O isotope geochemistry and stratigraphy of Precambrian and lower Paleozoic carbonate sequences from the Western Sierras Pampeanas of Argentina: tectonic implications. *Precambrian Res.* 131 (1–2), 55–71.
- Gallagher, K., Brown, R., Johnson, C., 1998. Fission track analysis and its applications to geological problems. *Ann. Rev. Earth Planet. Sci.* 26, 519–572.
- Giambiagi, L., Martínez, A.N., 2008. Permo-Triassic oblique extension in the Potrerillos-Uspallata area, western Argentina. *J. South Am. Earth Sci.* 26 (3), 252–260.
- Gleadow, A., Fitzgerald, P., 1987. Uplift history and structure of the Transantarctic Mountains: new evidence from fission track dating of basement apatites in the dry valleys area, southern Victoria Land. *Earth Planet. Sci. Letters* 82 (1–2), 1–14.
- Hourigan, J.K., Reiners, P.W., Brandon, M.T., 2005. U–Th zonation-dependent alpha-ejection in (U–Th)/He chronometry. *Geochim. Cosmochim. Acta* 69 (13), 3349–3365.
- Hurford, A.J., Green, P.F., 1983. The zeta age calibration of fission-track dating. *Chem. Geol.* 41 (0), 285–317.
- Jordan, T.E., Allmendinger, R.W., 1986. The sierras pampeanas of Argentina: a modern analogue of Rocky Mountain foreland deformation. *Am. J. Sci.* 286 (10), 737–764.
- Jordan, T.E., Isacks, B.L., Allmendinger, R.W., BREWER, J.A., Ramos, V.A., Ando, C.J., 1983. Andean tectonics related to geometry of subducted Nazca plate. *Geol. Soc. Am. Bull.* 94 (3), 341.
- Jordan, T.E., Zeitler, P., Ramos, V., Gleadow, A.J.W., 1989. Thermochronometric data on the development of the basement peneplain in the Sierras Pampeanas, Argentina. *J. South Am. Earth Sci.* 2 (3), 207–222.
- Keller, M., Buggish, W., Lehnert, O., 1998. The stratigraphic record of the Argentine Precordillera and its plate tectonic background. In: Pankhurst, R.J., Rapela, C.W. (Eds.), *The Proto-andean Margin of Gondwana*, vol. 142, pp. 35–56.
- Ketcham, R.A., 2005. Forward and Inverse modelling of low-temperature thermochronometry data. *Rev. Mineral. Geochem.* 58 (1), 275–314.
- Ketcham, R.A., Donelick, R.A., Carlson, W.D., 1999. Variability of apatite fission-track annealing kinetics III: extrapolation to geological time scales. *Am. Mineral.* 84, 1235–1255.
- Laslett, G., Green, P., Duddy, I., Gleadow, A., 1987. Thermal annealing of fission tracks in apatite 2. A quantitative analysis. *Chem. Geol. Isot. Geosci. Sect.* 65 (1), 1–13.
- Le Corre, C., Rossello, E., 1994. Kinematics of early paleozoic ductile deformation in the basement of NW Argentina. *J. South Am. Earth Sci.* 7 (3–4), 301–308.
- Löbens, S., Bense, F.A., Wemmer, K., Dunkl, I., Costa, C.H., Layer, P., Siegesmund, S., 2011. Exhumation and uplift of the Sierras Pampeanas: preliminary implications from K–Ar fault gouge dating and low-T thermochronology in the Sierra de Comechingones (Argentina). *Int. J. Earth Sci. (Geol. Rundsch)* 100 (2–3), 671–694. <http://dx.doi.org/10.1007/s00531-010-0608-0>.
- Löbens, S., Sobel, E.R., Bense, F.A., Wemmer, K., Dunkl, I., Siegesmund, S., 2013. Refined exhumation history of the Northern Sierras Pampeanas, Argentina. *Tectonics* 32, 453–472. <http://dx.doi.org/10.1029/2003Tect.20038>.
- Martino, R.D., 2003. Ductile deformation shear belts at Pampean Ranges near Córdoba, Central Argentina: a review. *Rev. Asoc. Geol. Argentina* 58 (4), 549–571.
- Meira, V.T., Campos Neto, M.d.C., González, P.D., Stipp Basei, M.Â., Varela, R., 2012. Ordovician klippen structures of the Sierra de Umango: new insights on Tectonic evolution of the Western Sierras Pampeanas, Argentina. *J. South Am. Earth Sci.* 37, 154–174.
- Morata, D., Castro Machuca, B., de Arancibia, G., Pontoriero, S., Fanning, C.M., 2010. Peraluminous Grenvillian TTG in the Sierra de Pie de Palo, Western Sierras Pampeanas, Argentina: petrology, geochronology, geochemistry and petrogenetic implications. *Precambrian Res.* 177 (3–4), 308–322.
- Mpodozis, C., Ramos, V.A., 1989. The Andes of Chile and Argentina, in: *Geology of the Andes and its Relation to Hydrocarbon and Mineral Resources*. In: Circumpacific Council for Energy and Mineral Resources. *Earth Sciences Series*, pp. 59–90.
- Mulcahy, S.R., Roeske, S.M., McClelland, W.C., Jourdan, F., Iriondo, A., Renne, P.R., Vervoort, J.D., Vujovich, G.I., 2011. Structural evolution of a composite middle to lower crustal section: the Sierra de Pie de Palo, northwest Argentina. *Tectonics* 30 (1). <http://dx.doi.org/10.1029/2009TC002656>.
- Mulcahy, S.R., Roeske, S.M., McClelland, W.C., Nomade, S., Renne, P.R., 2007. Cambrian initiation of the Las Pirquitas thrust of the western Sierras Pampeanas, Argentina: Implications for the tectonic evolution of the proto-Andean margin of South America. *Geology* 35 (5), 443.
- Müller, M., 1996. *Handbuch ausgewählter Klimastationen der Erde*, fifth ed. Universität Trier FB VI, Trier, Trier.
- Naipauer, M., Vujovich, G., Cingolani, C., McClelland, W., 2010. Detrital zircon analysis from the Neoproterozoic–Cambrian sedimentary cover (Cuyania terrane), Sierra de Pie de Palo, Argentina: Evidence of a rift and passive margin system? *J. South Am. Earth Sci.* 29 (2), 306–326.
- Pankhurst, R.J., Rapela, C.W., 1998. The proto-Andean margin of Gondwana: an introduction. *Geol. Soc. London Spec. Publ.* 142 (1), 1–9.
- Perez, A.M., Martínez, R., 1990. Modelación de cuerpos litosféricos en el área Pie de Palo, San Juan. In: XI Congreso Geológico Argentino, Actas, vol. 2, pp. 353–356.
- Ramos, V.A., 1988. The tectonics of central Andes: 30° to 33° latitude. *Spec. Paper Geol. Soc. Am.* 218, 31–54.
- Ramos, V.A., 2004. Cuyania, an exotic block to Gondwana: review of a Historical Success and the present problems. *Gondwana Res.* 7 (4), 1009–1026.
- Ramos, V.A., Cristallini, E.O., Pérez, D.J., 2002. The Pampean flat-slab of the Central Andes. *J. South Am. Earth Sci.* 15 (1), 59–78.
- Ramos, V.A., Dallmeyer, R.D., Vujovich, G., 1998. Time constraints on the early Palaeozoic docking of the Precordillera, central Argentina. *Geol. Soc. London Spec. Publ.* 142 (1), 143–158.
- Ramos, V.A., Folguera, A., 2009. Andean flat-slab subduction through time. *Geol. Soc. London Spec. Publ.* 327 (1), 31–54.

- Ramos, V.A., Vujovich, G.I., Dallmeyer, D., 1996. Los klippe y ventanas tectónicas de la estructura preándica de la sierra de Pie de Palo (San Juan): Edad e implicancias tectónicas. In: Proc. XIII Congreso Geológico Argentino Actas V, pp. 377–391.
- Ramos, V., Vujovich, G., 2000. Hoja Geológica 3169-IV San Juan, provincial de San Juan. Segemar. Boletín 243, 1–82.
- Rapela, C.W., Pankhurst, R.J., Casquet, C., Baldo, E., Saavedra, J., Galindo, C., 1998. Early evolution of the Proto-Andean margin of South America. *Geology* 26 (8), 707–710.
- Regnier, M., Chatelain, J.L., Smalley, R., Chiu, J.-M., Isacks, B.L., Araujo, M., 1992. Seismotectonics of Sierra Pie de Palo, a basement block uplift in the Andean foreland of Argentina. *Bull. Seismological Soc. Am.* 82 (6), 2549–2571.
- Reiners, P.W., Brandon, M.T., 2006. Using thermochronology to understand orogenic erosion. *Ann. Rev. Earth Planet. Sci.* 34, 419–466.
- Reiners, P.W., Spell, T.L., Nicolescu, S., Zanetti, K.A., 2004. Zircon (U–Th)/He thermochronometry: He diffusion and comparisons with $^{40}\text{Ar}/^{39}\text{Ar}$ dating. *Geochim. Cosmochim. Acta* 68 (8), 1857–1887.
- Rossello, E., Mozetic, M.E., 1999. Caracterización estructural y significado geotectónico de los depocentros cretácicos continentales del centro-oeste argentino. 5º Simposio sobre o Cretáceo do Brasil (Rio Claro). Boletim 5, 107–113.
- Roy, R., Cassard, D., Cobbold, P., Rossello, E., Billa, M., Bailly, L., Lips, A., 2006. Predictive mapping for copper–gold magmatic-hydrothermal systems in NW Argentina: Use of a regional-scale GIS, application of an expert-guided data-driven approach, and comparison with results from a continental-scale GIS. *Ore Geol. Rev.* 29 (3–4), 260–286.
- Sato, A.M., Tickyj, H., Llambías, E.J., Stipp Basei, M.A., González, P.D., 2004. Las Matras block, central Argentina (37°S – 67°W): the Southernmost Cuyania Terrane and its Relationship with the Famatinian Orogeny. *Gondwana Res.* 7 (4), 1077–1087.
- Sato, A., Tickyj, H., Llambías, E., Sato, K., 2000. The Las Matras tonalitic–trondhjemite pluton, central Argentina: Grenvillian-age constraints, geochemical characteristics, and regional implications. *J. South Am. Earth Sci.* 13 (7), 587–610.
- Schmidt, C., Astini, R., Costa, C., Gardini, C., Kraemer, P., 1995. Cretaceous rifting, alluvial fan sedimentation, and Neogene inversion, southern Sierras Pampeanas, Argentina. In: Tankard, A.J., Suárez Soruco, R., Welsink, H.J. (Eds.), *Petroleum Basins of South America*, vol. 62. Published jointly by the American Association of Petroleum Geologists, Yacimientos Petrolíferos Fiscales Bolivianos, Academia Nacional de Ciencias de Bolivia, Tulsa, Okla., pp. 341–358.
- Simpson, C., Law, R.D., Gromet, L., Miro, R., Northrup, C., 2003. Paleozoic deformation in the Sierras de Córdoba and Sierra de Las Minas, eastern Sierras Pampeanas, Argentina. *J. South Am. Earth Sci.* 15 (7), 749–764.
- Sobel, E.R., Strecker, M.R., 2003. Uplift, exhumation and precipitation: tectonic and climatic control of Late Cenozoic landscape evolution in the northern Sierras Pampeanas, Argentina. *Basin Res.* 15 (4), 431–451. <http://dx.doi.org/10.1046/j.1365-2117.2003.00214>.
- Stockli, D.F., Farley, K.A., Dumitru, T.A., 2000. Calibration of the apatite (U–Th)/He thermochronometer on an exhumed fault block, White Mountains, California. *Geology* 28, 983–986.
- Thomas, W.A., Astini, R.A., 2003. Ordovician accretion of the Argentine Precordillera terrane to Gondwana: a review. *J. South Am. Earth Sci.* 16 (1), 67–79.
- van Staal, C., Vujovich, G., Currie, K., Naipauer, M., 2011. An Alpine-style Ordovician collision complex in the Sierra de Pie de Palo, Argentina: Record of subduction of Cuyania beneath the Famatinian arc. *J. Struct. Geol.* 33 (3), 343–361.
- Varela, R., Basei, M.A.S., González, P.D., Sato, A.M., Naipauer, M., Campos Neto, M., Cingolani, C.A., Meira, V.T., 2011. Accretion of Grenvillian terranes to the southwestern border of the Río de la Plata craton, western Argentina. *Int. J. Earth Sci. (Geol. Rundsch)* 100 (2–3), 243–272.
- Varela, R., Dalla Salda, L.H., 1992. Geocronología Rb–Sr de metamorfitas y granitoídes del tercio sur de la Sierra de Pie de Palo, San Juan, Argentina. *Rev. Asoc. Geol. Argentina* 47, 271–275.
- Vita-Finzi, C., 2009. Pie de Palo, Argentina: a cataclastic diapir. *Geomorphology* 104 (3–4), 317–322.
- Vujovich, G.I., 2003. Metasedimentos siliciclasticos proterozoicos en la Sierra de Pie de Palo, San Juan: Procedencia y ambiente tectónico. *Rev. Asoc. Geol. Argentina* 58 (4), 608–622.
- Vujovich, G.I., Kay, S.M., 1998. A Laurentian? Grenville-age oceanic arc/back-arc terrane in the Sierra de Pie de Palo, Western Sierras Pampeanas, Argentina. *Geol. Soc. London Spec. Public.* 142 (1), 159–179.
- Vujovich, G.I., van Staal, C.R., Davis, W., 2004. Age Constraints on the Tectonic Evolution and Provenance of the Pie de Palo Complex, Cuyania Composite Terrane, and the Famatinian Orogeny in the Sierra de Pie de Palo, San Juan, Argentina. *Gondwana Res.* 7 (4), 1041–1056.
- Wolf, R., Farley, K.A., Kass, D., 1998. Modeling of the temperature sensitivity of the apatite (U–Th)/He thermochronometer. *Chemical Geol.* 148 (1–2), 105–114.
- Wolf, R., Farley, K.A., Silver, L., 1996. Helium diffusion and low-temperature thermochronometry of apatite. *Geochim. Cosmochim. Acta* 60 (21), 4231–4240.
- Yáñez, G.A., Ranero, C.R., Huene, R., von, Díaz, J., 2001. Magnetic anomaly interpretation across the southern central Andes (32° – 34°S): the role of the Juan Fernández Ridge in the late Tertiary evolution of the margin. *J. Geophys. Res.* 106 (B4), 6325–6345.
- Zapata, T., 1998. Crustal structure of the Andean thrust front at 30°S latitude from shallow and deep seismic reflection profiles, Argentina. *J. South Am. Earth Sci.* 11 (2), 131–151.